

Molecular Imaging of Influenza and Other Emerging Respiratory Viral Infections

Mike Bray,¹ James Lawler,³ Jason Paragas,³ Peter B. Jahrling,³ and Daniel J. Mollura²

¹Division of Clinical Research, National Institute of Allergy and Infectious Diseases, and ²Center for Infectious Disease Imaging, Department of Radiology and Imaging Sciences, Clinical Center, National Institutes of Health, Bethesda, and ³Integrated Research Facility, National Institute of Allergy and Infectious Diseases, National Institutes of Health, Fort Detrick, Maryland

Research on the pathogenesis and therapy of influenza and other emerging respiratory viral infections would be aided by methods that directly visualize pathophysiologic processes in patients and laboratory animals. At present, imaging of diseases, such as swine-origin H1N1 influenza, is largely restricted to chest radiograph and computed tomography (CT), which can detect pulmonary structural changes in severely ill patients but are more limited in characterizing the early stages of illness, differentiating inflammation from infection or tracking immune responses. In contrast, imaging modalities, such as positron emission tomography, single photon emission CT, magnetic resonance imaging, and bioluminescence imaging, which have become useful tools for investigating the pathogenesis of a range of disease processes, could be used to advance in vivo studies of respiratory viral infections in patients and animals. Molecular techniques might also be used to identify novel biomarkers of disease progression and to evaluate new therapies.

The public health importance of novel respiratory viral infections has been underlined during the past decade by the emergence of H5N1 avian influenza in Southeast Asia, the epidemic of severe acute respiratory syndrome (SARS), and the pandemic of swine-origin H1N1 influenza that began in early 2009. As each new disease has been identified, physicians have made use of chest radiography and computed tomography (CT) to characterize pulmonary morphologic changes in patients at the time of presentation and in cases of severe illness and to identify prognostic markers of

disease progression [1–5]. However, although these radiographic methods are useful for clinical management, their ability to elucidate underlying pathologic mechanisms is much more limited. Research would, therefore, benefit from techniques that could image physiologic processes in patients or in laboratory animals over the course of illness. In this regard, the use of molecular imaging methods could markedly enhance the ability to study the pathophysiology of influenza and other emerging respiratory viral infections.

Molecular imaging has been defined by the Society of Nuclear Medicine as “the visualization, characterization, and measurement of biological processes at the molecular and cellular levels in humans and other living systems” [6]. It may use multiple imaging modalities, with either 2-dimensional or 3-dimensional images, and can involve quantification of data over time. The key factor is that data are obtained through the interaction of the imaging

mechanism with cellular or subcellular processes, such as enzymatic modification or receptor binding. [7, 8]. Single-photon emission CT (SPECT) and positron emission tomography (PET) can be used for molecular imaging by using radiolabeled probes to detect the presence of specific target molecules or biochemical reactions in sites of interest. In addition, some applications of magnetic resonance imaging (MRI) use differences in susceptibilities to magnetic fields to label cells and differentiate surrounding tissues. Bioluminescence imaging (BLI) can also elucidate pathophysiologic processes in murine models of human illness, using visible light produced by luciferase or other recombinant reporter molecules.

In this article, we describe how molecular imaging methods could be used to study respiratory viral infections in patients and laboratory animals. The first section assesses the capabilities and limitations of current radiographic methods, by reviewing typical chest

Received 25 October 2010; accepted 13 December 2010.
Potential conflicts of interest: none reported.

Correspondence: Mike Bray, MD, Div of Clinical Research, National Institute of Allergy and Infectious Diseases, National Institutes of Health, Bethesda, MD 20892 (mbray@niaid.nih.gov).

The Journal of Infectious Diseases 2011;203:1348–59
© The Author 2011. Published by Oxford University Press on behalf of the Infectious Diseases Society of America. All rights reserved. For Permissions, please e-mail: journals.permissions@oup.com
0022-1899 (print)/1537-6613 (online)/2011/20310-0002\$14.00
DOI: 10.1093/infdis/jir038

radiograph and CT findings in swine-origin H1N1 influenza, H5N1 avian influenza, and SARS. We then describe how SPECT, PET, MRI, and BLI could be used to enhance our understanding of the underlying mechanisms of these disease processes.

CHEST RADIOGRAPH AND CT IMAGING OF RESPIRATORY VIRAL INFECTIONS

Clinical radiography assesses the physical characteristics of body tissues based on the attenuation of high-energy photons (X-rays) as they pass through regions of differing density. Soon after X-rays were discovered in 1895, the human thorax was found to be an excellent substrate for imaging, because the air-filled lungs provided a low-density background against which areas of consolidation and other structural changes could be visualized. The value of chest radiography for assessing the severity of respiratory tract infections was firmly established during the 1918 influenza pandemic, in which the new radiologic capabilities were widely implemented to

study patients and to correlate imaging with pathologic and clinical findings [9]. At the same time, it was recognized that the radiographic changes typical of severe influenza were also observed in other conditions, both infectious and noninfectious. The ability of chest radiographs to detect and discriminate disease processes was also restricted by overlapping projections of soft tissues. Although this problem was partly mitigated by the development of CT, which enabled major advances in image resolution, the sensitivity and specificity of radiographic imaging remain limited by the absence of unique features to distinguish infection from inflammation and by the lack of standardized scoring systems for disease severity [9, 10]. The value of chest radiographs and CT for research is also restricted by the difficulty of obtaining direct radiologic-pathologic correlation, because lung tissue samples from patients with influenza are only examined when a case ends in death, followed by autopsy.

The capabilities and limitations of radiography for the study of respiratory viral infections are illustrated by reports from past disease outbreaks and the

swine-origin H1N1 influenza pandemic [10–14]. In cases of mild, self-limited illness, in which lesions apparently remain localized to the upper respiratory tract (Figure 1D), the chest radiograph is either normal or displays only minor changes. The development of more severe disease is typically marked by the appearance of multiple patchy densities in one or both lungs, in a multilobar peripheral distribution (Figure 1A). By CT, these areas are termed ground-glass opacities (GGO) because of the hazy density of the lesions, in which the margins of bronchi and blood vessels are partially visible (Figure 1B). Autopsy findings suggest that GGO correspond to foci of viral pneumonitis and/or diffuse alveolar damage (Figure 1E). However, GGO are also seen in a variety of other pulmonary diseases, both infectious and noninfectious, in which they may reflect partial airspace filling, interstitial cellular infiltration or edema, capillary congestion, or a combination of these factors [10, 12, 14]. CT imaging of some patients with swine-origin H1N1 influenza has also shown consolidative patterns, in which the increased lesion density obscures all

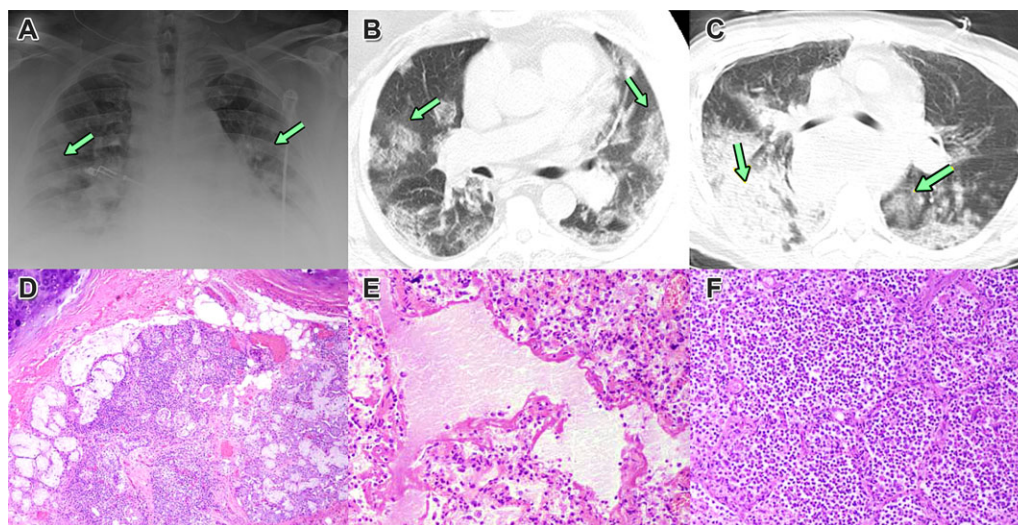


Figure 1. Radiographs and histopathologic examination of lung tissues at autopsy of patients fatally infected with pandemic swine-origin H1N1 influenza. *A*, Chest radiograph on day 5 of illness, showing multiple, bilateral opacities (arrows). *B*, CT of the same patient, showing multifocal, patchy ground-glass opacities. *C*, CT of a different patient, showing areas of denser consolidation consistent with bacterial pneumonia. *D*, Section of trachea showing inflammation of submucosal glands. *E*, Section of lung showing diffuse alveolar damage with hyaline membrane formation. *F*, Section of lung showing a massive infiltrate of neutrophils, consistent with bacterial pneumonia. (From [12] and [14], with permission.)

parenchymal structures except for some traversing open airways (air bronchograms), consistent with either severe viral injury or bacterial pneumonia (Figure 1C, 1E) [12, 15].

In contrast to influenza, in which fatal disease generally occurs only in infants, older persons, and persons with underlying medical conditions, severe cases of SARS frequently occurred in previously healthy individuals. However, the spectrum of radiographic changes seen in the epidemic largely resembled that observed in the swine-origin H1N1 influenza pandemic (Figure 2A, B) [16]. In both influenza and SARS, patients with severe illness show patchy, bilateral infiltrates by chest radiograph and multifocal GGO on CT. Because the radiographic findings are not specific, a diagnosis of SARS could only be made if a patient gave a history of contact with a person with a known case. However, radiography still contributed to medical management by identifying patients in need of intensive supportive care and by assessing their response to therapy [1, 17]. In contrast to severely ill patients with influenza, in many of whom influenza progressed to bacterial pneumonia, fatal cases of SARS were typically characterized by the progressive expansion of areas of GGO to involve both lungs [17]. In the only radiographic study in laboratory animals, pulmonary airspace opacities were observed in cynomolgus macaques infected with the SARS coronavirus by the respiratory route (Figure 3), but a radiologic-pathologic correlation was not obtained [18].

Similar to the situation with SARS and severe swine-origin H1N1 influenza, chest radiographs of patients with H5N1 avian influenza show the early development of multiple, bilateral patchy opacities, which in fatal cases, progress rapidly to acute respiratory distress syndrome (ARDS) (Figure 4) [3]. The rapid development of severe, diffuse pulmonary parenchymal dysfunction is thought to reflect the

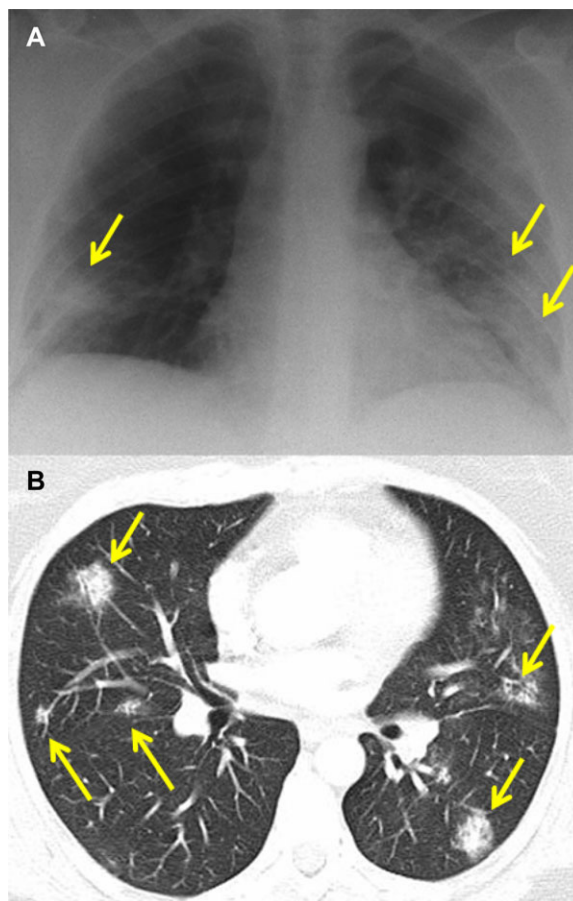


Figure 2. Chest radiograph (A) and CT (B) of a 46-year-old woman with SARS on day 12 of hospitalization. The radiograph shows bilateral, multifocal opacities (arrows), which appear on CT as multiple subpleural areas of ground-glass attenuation. (Courtesy of Dr. Narinder Paul, Toronto.) The similarity of these changes to those seen in swine-origin H1N1 influenza (Figure 1) illustrates the nonspecificity of radiographic findings in viral infections of the respiratory tract.

propensity of the H5N1 virus to infect alveolar lining cells, in contrast to the tropism of seasonal influenza A viruses for the tracheobronchial epithelium, coupled with an intense inflammatory response [19].

The above discussion has shown that, although radiographic methods are capable of providing detailed images of the morphologic alterations that accompany severe respiratory viral infections, they provide little or no information on

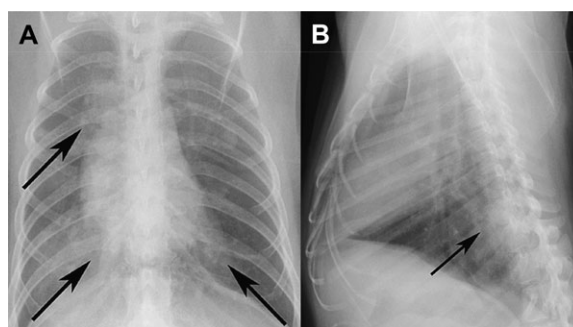


Figure 3. Posterior-anterior and lateral radiographs of a cynomolgus macaque 6 days after infection with SARS coronavirus by the intranasal and intrabronchial routes, showing multiple areas of pulmonary opacification (arrows). (From [18].)

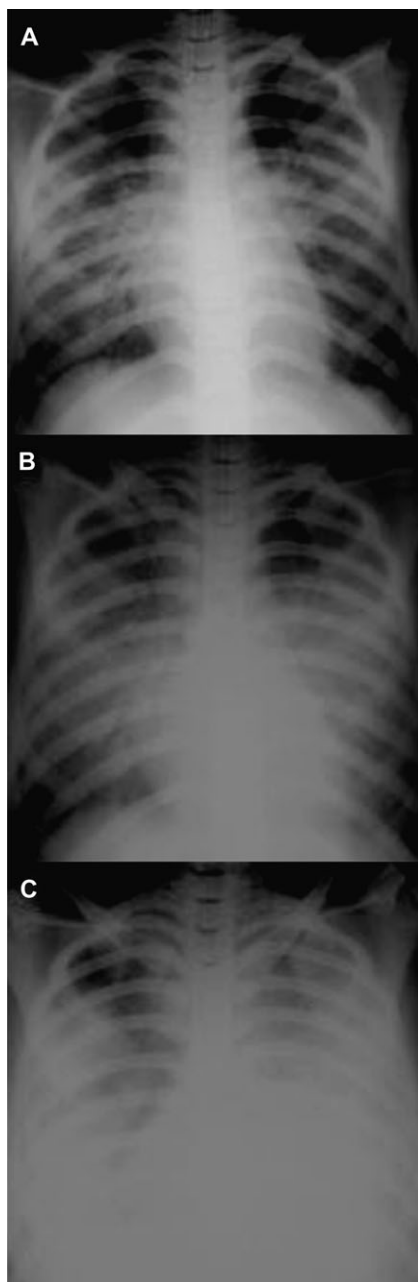


Figure 4. Sequential radiographs of a 22-year-old man with H5N1 avian influenza. The film on hospital admission (*A*) shows bilateral perihilar patchy opacities with air bronchograms. Two days later (*B*), there was bilateral multifocal consolidation. On day 4, the patient showed worsening respiratory failure with features suggestive of ARDS. (From [3], with permission.)

the pathophysiologic mechanisms responsible for such changes. In particular, it is not known whether influenza and other viral infections are initially limited

to the upper respiratory tract or whether severe pulmonary involvement is the result of a more diffuse initial disease process. Similarly, the mechanisms responsible for the development of pulmonary infiltrates and GGO have not been identified, and it is not known to what extent respiratory dysfunction is the result of viral infection and injury of the respiratory tract epithelium or is induced by the local or systemic release of inflammatory mediators. The factors that predispose some patients to the development of fatal bacterial superinfection are also poorly understood. Imaging methods that are not based on tissue structural changes, but on the detection of specific biochemical processes, may be able to answer such questions.

MOLECULAR IMAGING

Historically, a major goal of imaging has been to facilitate medical treatment decisions by differentiating infectious from inflammatory processes (eg, osteomyelitis from aseptic inflammation) [20]. In recent years, much of this effort has focused on the characterization of host immune responses through molecular applications of SPECT, PET, and MRI; many of these approaches could potentially be used to image respiratory viral infections (Table 1). Ideally, researchers would also use molecular imaging to directly visualize viral infections, in the way that SPECT is now being used to detect experimental mycobacterial infections with use of a bacterial thymidine kinase (TK) enzyme as the reporter molecule (Figure 5) [30].

In the case of viral infections, pathogen-specific imaging would rely either on the construction of recombinant viruses encoding reporter molecules, as has been accomplished for BLI, or on the development of radiolabeled probes that are selectively retained at sites of infection (Table 2). If techniques can be devised to specifically image viral infections in large animals or humans, the

eventual goal will be to visualize host responses and viral replication simultaneously, to determine the relationship between the spread of the pathogen and processes, such as the release of proinflammatory mediators, the influx of inflammatory cells, apoptosis of infected or bystander cells, and changes in vascular function. In the following sections, we review the basic principles of SPECT, PET, MRI and BLI and discuss how they could be used to enhance our understanding of influenza and other respiratory viral infections.

Radionuclide Imaging

SPECT and PET are based on the selective retention of radiotracer molecules at sites of biological interest through a broad range of mechanisms including either as a result of high-affinity binding to a chosen molecular target or through trapping in cells by mechanism pathways such as modification by a specific enzyme. PET imaging probes emit positrons, which travel a short distance in tissues before undergoing annihilation, producing 2 high-energy photons traveling in 180° opposite directions that strike surrounding detectors simultaneously. By using highly energetic photons of a single frequency, PET reduces soft-tissue attenuation, scatter, and noise. However, a limiting factor in PET resolution is the distance that the positron must travel through tissues before undergoing annihilation. In contrast, the various radiotracers used for SPECT imaging release single photons, with a range of energies depending on the decay characteristics of the radionuclide.

Although SPECT has traditionally been considered to be less quantitative and more subject to soft-tissue attenuation than PET, its use for infectious disease research is being enhanced by improved collimation, the use of CT for attenuation correction, and evolving quantitative techniques. Although not all SPECT radiotracers are used for molecular imaging, SPECT offers a wide variety of probes, because it is not limited by

Table 1. Molecular Imaging Techniques That Are Currently Being Used to Study Host Responses to Cancer, Inflammatory and Autoimmune Diseases, and Other Medical Conditions, Which Could Also Be Applied to Research on Respiratory Viral Infections

Host response	Imaging methods	Current status
Apoptosis resulting from infection or inflammation	SPECT imaging with ^{99m}Tc radiolabeled annexin-V for pulmonary disease [21].	Laboratory animals
Triggering of type I interferon response	BLI imaging of transgenic mice in which luciferase expression is driven by an IFN-beta promoter [22].	Laboratory animals
Identification of sites of inflammation	Intravenous infusion of ^{67}Ga -citrate, which binds to transferrin and lactoferrin and localizes to sites of increased vascular flow and permeability [23]. Intravenous infusion of ^{111}In -labeled immunoglobulin, followed by planar gamma camera and SPECT imaging [23]. Intravenous infusion of ^{18}F -FDG, followed by PET imaging to detect foci of increased glycolytic activity [24]. <i>In vitro</i> labeling of leukocytes with ^{111}In oxine or leukocyte labeling with ^{99m}Tc -exametazime (also known as ^{99m}Tc -HMPAO), for planar gamma camera imaging or SPECT [25, 26]. Identification of activated monocytes/macrophages by infusion of superparamagnetic iron oxide particles, followed by MRI [25].	Clinical practice, Preclinical research, Laboratory animals
Alterations in the size and structure of regional lymph nodes	Characterization of lymph node structure by infusion of superparamagnetic iron oxide particles, followed by MRI [26].	Laboratory animals
Activation of vascular endothelium	Detection of increased cell-surface ICAM-1 or E-selectin expression with radiolabeled antibodies [27] [28]. Detection of increased E-selectin expression by MR, using superparamagnetic iron oxide nanoparticles labeled with specific antibody [29].	Laboratory animals

NOTE. Column 3 indicates whether the procedures are in clinical use, are being employed in preclinical studies in humans, or are limited to imaging of laboratory animals.

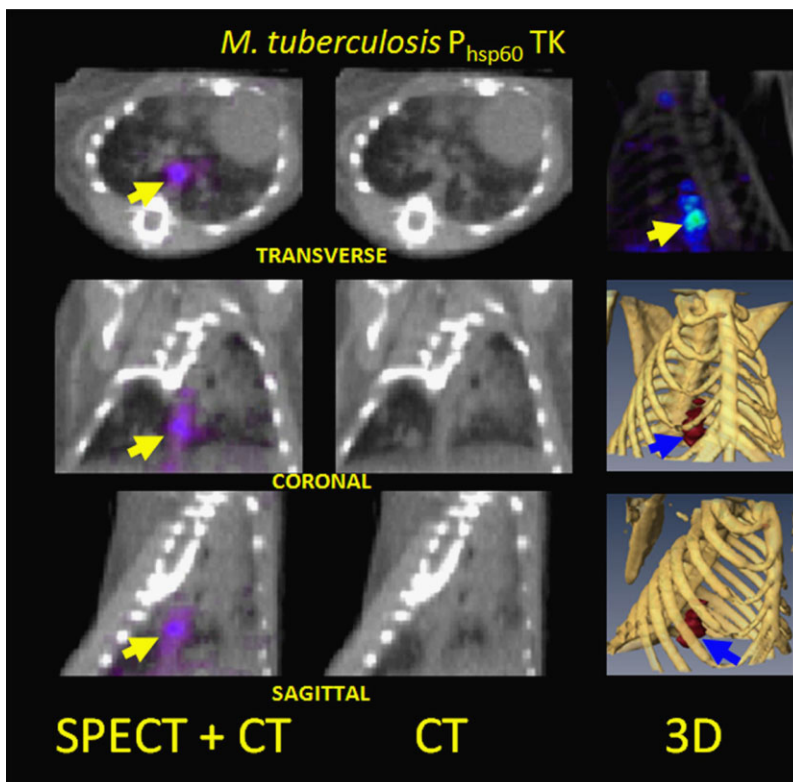


Figure 5. SPECT/CT images of the thorax of a mouse 6 weeks after low-dose aerosol infection with recombinant *M. tuberculosis*, in which a bacterial TK gene is under the control of the strong, constitutive P_{hsp60} promoter. The probe is 1-(2-deoxy-2-fluoro- β -D-arabinofuranosyl) - 5-[^{125}I]-iodouracil (^{125}I -FIAU), which is preferentially phosphorylated by the bacterial TK over the host cell enzyme to produce SPECT signal localizing to pulmonary granulomas (arrows). (From [30].)

a requirement for positron decay. Moreover, as a cross-sectional technique, SPECT provides significant advantages over planar nuclear medicine imaging for locating sites of disease. For example, whole antibodies or antibody fragments labeled with ^{99m}Tc or ^{111}In can be imaged with SPECT for a broad range of potential infectious disease applications.

The most widely used PET radiotracer is ^{18}F -fluorodeoxyglucose (FDG). Because deoxyglucose is taken up by cells and phosphorylated but not further metabolized, the radiotracer is selectively trapped in cells with high rates of glycolysis. FDG - PET imaging has a flourishing oncologic literature, based on the detection of active neoplasms with elevated glycolysis by combining PET with CT, which has greater sensitivity and specificity than either method alone. In contrast, relatively few data have yet been published to support a role for FDG - PET and/or CT in infectious diseases imaging. In clinical practice, FDG - PET and/or CT can also visualize inflammatory processes, both infectious

Table 2. Hypothetical Targets for Molecular Imaging in the Replication Cycle of Influenza A Viruses and the SARS Coronavirus

Target	Potential imaging methods	
	Influenza A viruses	SARS coronavirus
Binding of virion to cell-surface receptor	PET or SPECT imaging using radiolabeled lectins or viral HA molecules as probes. BLI of infection by a GFP- or luciferase-encoding virus [32].	BLI of infection by a GFP- or luciferase-encoding virus [33].
Fusion and entry into cell	PET or SPECT imaging using radiolabeled adamantanes, which bind specifically within the M2 ion channel [34].	PET or SPECT imaging using radiolabeled peptide inhibitors of viral membrane fusion [35].
Transcription and genome replication	PET or SPECT imaging using a recombinant virus encoding the HSV TK, or using a radiolabeled non-nucleoside RNA polymerase inhibitor as tracer.	PET or SPECT imaging using a recombinant virus encoding the HSV TK, or using a radiolabeled non-nucleoside RNA polymerase inhibitor as tracer.
Processing of viral proteins and virion assembly		PET or SPECT imaging using a radiolabeled protease inhibitor as a tracer [36].
Budding and exit of virus particles	PET or SPECT imaging using radiolabeled antibodies that bind to viral antigens on the cell surface, or a radiolabeled neuraminidase inhibitor.	PET or SPECT imaging using radiolabeled antibodies that bind to viral antigens on the cell surface [37].

NOTE. For BLI, sites of replication can be identified through the expression of a virus-encoded luciferase, GFP or other reporter molecule, as has been shown for an influenza virus encoding a chimeric NS1-GFP protein [31]. Virus-specific imaging with PET or SPECT might make use of a radiolabeled probe that binds with high affinity to a virus-specific molecule, or is selectively modified by a virus-encoded enzyme, causing it to be retained within infected cells.

and noninfectious, via nonspecific uptake of the tracer by multiple types of white blood cells, including lymphocytes and neutrophils. Therefore, FDG - PET and/or CT can theoretically be a useful tool for measuring inflammatory responses to infection [38]. For example, FDG has been used to visualize the response to the introduction of endotoxin into the lungs of human volunteers (Figure 6) [39, 40]. This suggests that FDG - PET could be particularly useful for imaging the inflammatory response to severe respiratory viral

infections, because studies of human cases and experimental models in mice and ferrets indicate that acute inflammatory responses play a critical role in the severe respiratory dysfunction induced by the 1918 H1N1 and the H5N1 avian influenza viruses and by the SARS coronavirus [19, 41–46]. Radionuclide imaging of experimental influenza or SARS coronavirus infections could help to resolve the question of whether anti-inflammatory therapies are beneficial or harmful for these conditions [47–51].

FDG-PET and/or CT were recently used to study a patient with severe influenza, showing that areas of GGO seen by CT were characterized by increased radiotracer uptake (Figure 7) [52]. The same authors have also found that, in patients with acute lung injury and ARDS from causes other than viral infection, the metabolic rate of pulmonary tissues is markedly increased, even when CT shows them to be normally aerated [53]. This work suggests that FDG - PET quantitation of inflammation in infected animals could be experimentally compared with measurements of viral replication, cellular markers, and gene expression to identify relationships among these factors and pulmonary parenchymal injury.

Because intravenously administered FDG is taken up and trapped nonspecifically by a wide range of white blood cells, efforts are under way to label specific populations of white blood cells in vitro. In the case of acute infection, in vitro labeling of neutrophils could be a useful method of tracking host responses [24, 54]. For example, a ⁶⁴Cu-labeled peptide that targets the formyl peptide receptor on neutrophils has been

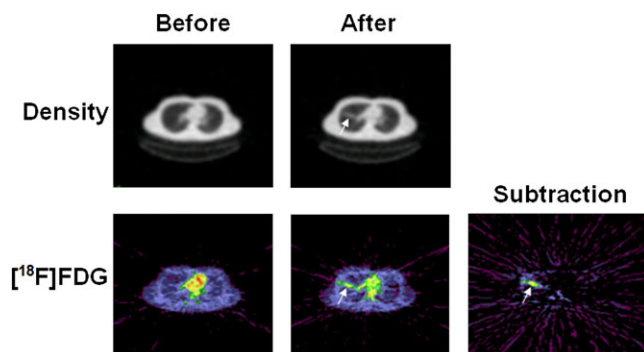


Figure 6. CT (upper row) and ¹⁸F-FDG-PET images of the lungs of a human volunteer before and 24 hours after an intrabronchial installation of endotoxin. The subtraction image shows an area of tracer retention representing an acute inflammatory response. Red indicates the highest and blue the lowest level of activity. (From [39], with permission.)

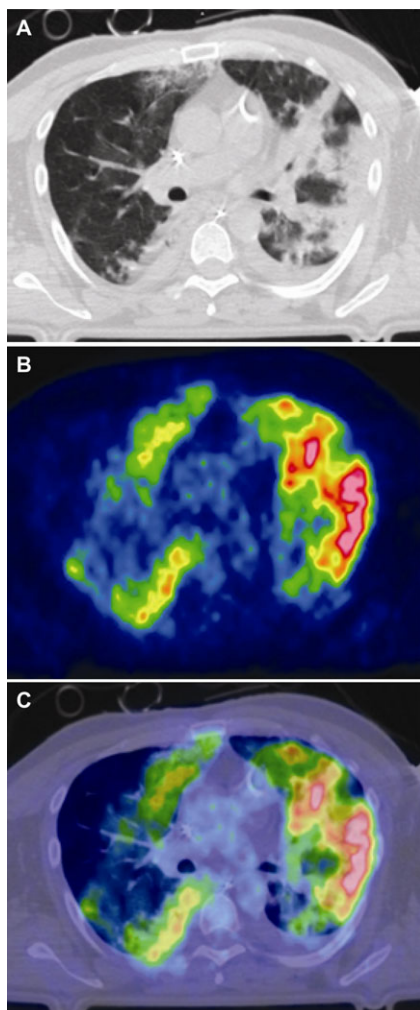


Figure 7. Chest CT (A), ^{18}F -FDG-PET scan (B), and fused image (C) of a patient with severe swine-origin H1N1 influenza and ARDS. The PET image shows increased glucose metabolism, both in areas that contain infiltrates by CT and in regions of apparently normal aeration. Red indicates the highest and blue the lowest level of radiotracer activity. (Courtesy of Giacomo Bellani.)

used to image bacterial infections in mice [55]. Key issues include demonstrating the stability of the neutrophil-peptide complex, which affects the localization of a molecular process if the radioactive molecule fails to remain attached to the target peptide, and studying the effect on tracer uptake of increased perfusion in areas of infection [55].

Because the techniques just described cannot reliably distinguish between infection and other inflammatory

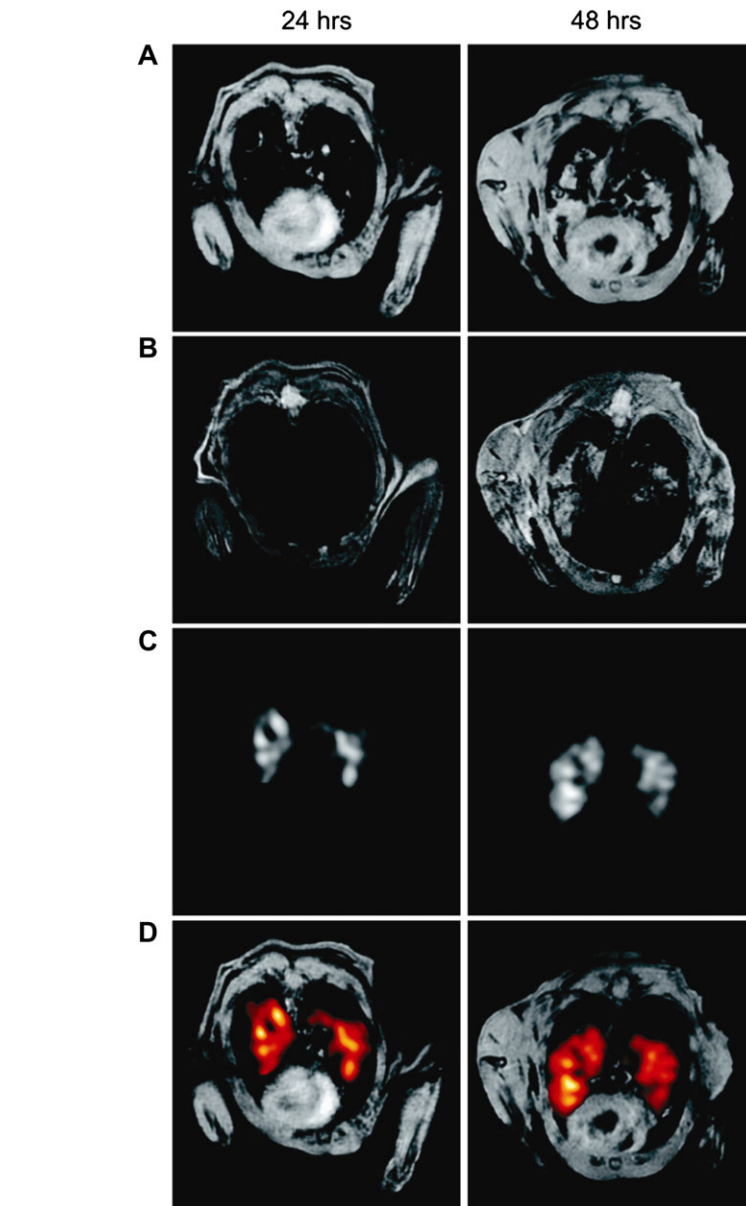


Figure 8. Identification by MRI of areas of inflammation in the lungs of a mouse 24 and 48 hours after an intratracheal inoculation of lipopolysaccharides, based on the uptake of ^{19}F -labeled emulsified perfluorocarbons, which are phagocytized by monocytes and macrophages. A and B, ^1H gradient echo images of the thorax. C, ^{19}F MRI. D, Superimposed images, with sites of perfluorocarbon uptake highlighted in red. (From [67], with permission.)

processes, there is a need for methods that could specifically detect viral replication and track the spread of a pathogen in the respiratory tract. One possible approach would be to design radio-labeled probes that bind with high affinity to virus-encoded molecules or that are substrates for a virus-encoded enzyme (Table 2). An example of the latter is the herpesviral TK, which

phosphorylates thymidine analogues that are not substrates for the host enzyme. Compounds, such as acyclovir and its analogues, can therefore be used both as antiviral drugs for the treatment of herpesviral infections and as radio-labeled tracers to detect sites of replication or recombinant TK expression [56]. The method has been used to image experimental herpesviral infections of

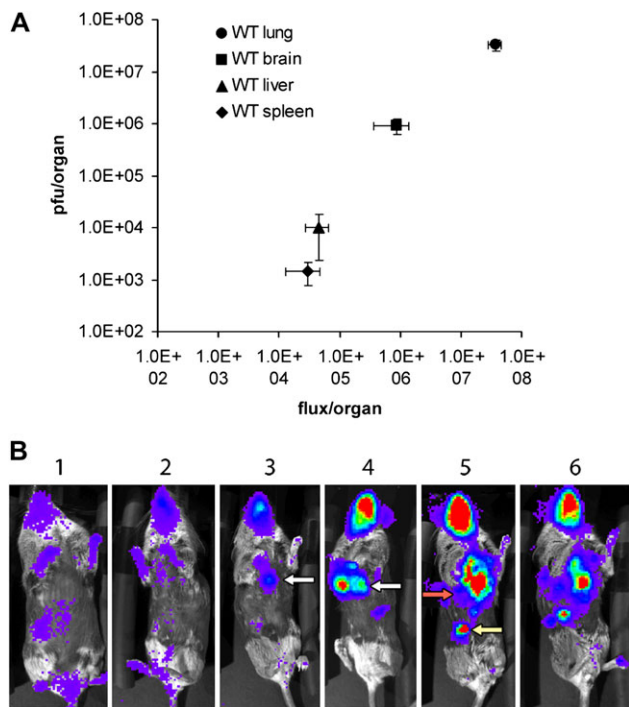


Figure 9. A, correlation of photon flux with viral titers in the organs of interferon- α receptor knockout mice infected intranasally with a recombinant vaccinia virus encoding firefly luciferase. The animals were killed on day 7 after infection, and tissue samples were analyzed for luciferase activity and viral titer. B, BLI of the infected mice, showing the progression of infection over time (days). Red indicates the highest and blue the lowest level of radiotracer activity. (From [75], with permission.)

tumors, but its use for visualizing herpesviral encephalitis has been limited by the requirement for the probe to penetrate the blood-brain barrier [57–59].

The published literature has not yet established the use of radiolabeled antiviral drugs as probes to image influenza or SARS, but opportunities might exist to use amantadine and rimantadine, which inhibit influenza viral replication by selectively occupying the M2 ion channel; oseltamivir and zanamivir, which bind to the active site of the influenza neuraminidase; and experimental drugs that inhibit the SARS coronavirus protease as imaging agents [34, 36]. PET has been used to image the distribution of radiolabeled oseltamivir in uninfected mice and of inhaled zanamivir in healthy human volunteers [60, 61]. It is interesting to speculate that these radiolabeled drugs could also be used to identify the distribution of

influenza virus in the respiratory tract of patients with influenza, unless their distribution would essentially localize nonspecifically to areas of increased perfusion, as has been observed for radiolabeled ciprofloxacin in experimental bacterial infections [62].

Magnetic Resonance Imaging

In MRI, exposure of the body to a combination of a strong magnetic field and pulses of radio-frequency energy induces signals that reflect the local molecular environment. In addition to providing detailed structural images, MRI can obtain information on physiologic processes through the use of contrast agents, such as superparamagnetic iron oxide (SPIO) particles, to label immune cells and the analysis of spectral data to detect and quantify specific substances in tissues. The use of MRI for the study of pulmonary disease has been significantly

more limited than CT because of several challenges, including cardiac and respiratory motion, the low water content of pulmonary parenchyma, and the variable magnetic susceptibility at alveolar and bronchial structure interfaces, which produces short T2 and T2* relaxation times, lowering the signal-to-noise ratio [63]. However, technical innovations, such as respiratory gating and adjusted MRI sequences, are addressing these challenges to image pulmonary infections [64–66].

MRI is now being used to track the development of pulmonary lesions and characterize inflammatory responses in murine models of bacterial infection (Figure 8A) [67–70]. Although MRI has been used to study the effects of influenza on the central nervous system and the heart, it has yet to be applied in published research on pulmonary influenza or other respiratory viral infections. However, advances in pulmonary MRI and MRI-compatible cell labeling are providing a unique opportunity for these studies. For example, inflammatory cells loaded *ex vivo* with antiviral drugs or nanoparticles have been demonstrated to localize to sites of infection [71, 72]. SPIO particles, which cause local magnetic susceptibility artifacts, are particularly useful for studying inflammatory processes, because they are detectable as dark (hypointense) regions much larger than the particles themselves, rendering them visible even when only a few cells are labeled (Figure 8B) [73]. Although promising for identifying areas of inflammation in solid organs, such as the brain, these methods may prove to be less useful for studying respiratory tract infections, because dark areas of diminished signal intensity at sites of SPIO particle uptake may resemble normal lung.

Bioluminescence Imaging

Because it uses relatively inexpensive detection equipment and does not involve radioactivity, BLI is the molecular imaging method most accessible to

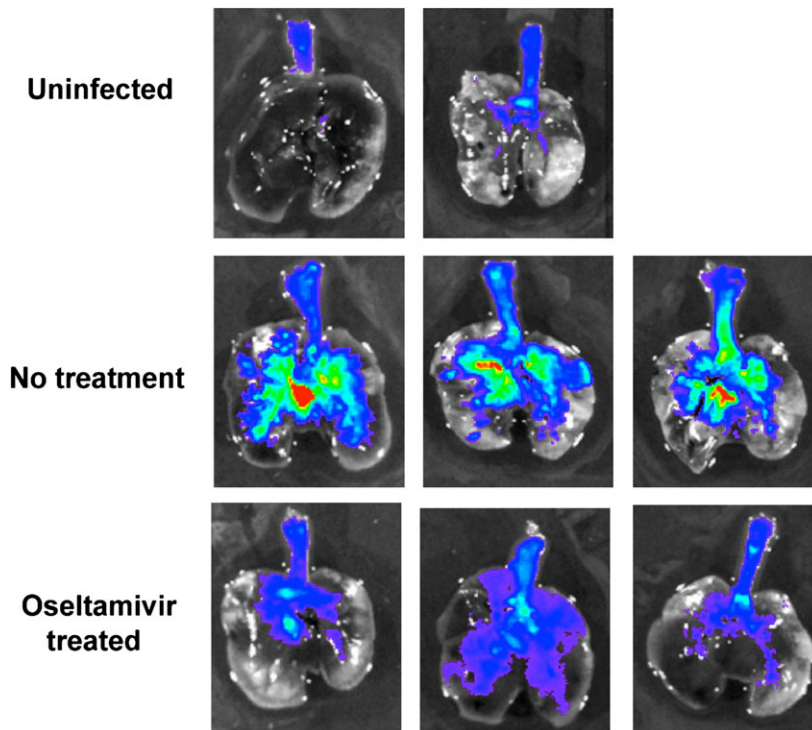


Figure 10. Ex vivo imaging of the distribution of a GFP-encoding influenza A virus in the lungs of mice 2 days after intranasal inoculation, without or with oseltamivir therapy. In the treated animals, the signal is almost entirely low-level (blue) and is localized principally to the central large airways, while the photon flux is more intense and diffuse in the untreated mice. (From [31], with permission.)

bench researchers. The technique is based on the emission of photons of visible or near-infrared light by firefly luciferase when it is exposed to an injected bolus of its natural substrate, luciferin [74]. Because photons in this energy range are quickly absorbed as they pass through tissues, BLI studies can only be performed in small animals (predominantly in mice) with organs of interest within a few millimeters of the skin surface.

Most investigators who have used BLI to visualize viral replication have inserted a luciferase gene into the genome of the agent of interest, a procedure that is quite straightforward for large DNA viruses, such as the poxviruses. In the case of vaccinia virus infections of the respiratory tract, the photon flux from the lungs has been shown to correlate directly with tissue viral titers, making it possible to both visualize and quantitate viral replication in living animals over the entire course

of illness (Figure 9) [76, 77]. Thus, BLI has the potential to supplement or even replace some traditional research methods in which data on viral replication could only be obtained by infecting a large number of mice, sacrificing cohorts at various time points, collecting tissue samples, and determining viral titers.

The insertion of a reporter gene is more challenging for a small RNA virus such as influenza. However, a recombinant influenza A virus encoding a chimeric NS1-green fluorescent protein (GFP) molecule has been successfully generated and used to image the distribution of virus in the lungs of infected mice [31]. Because of the short tissue penetration of UV light and the presence of background autofluorescence, imaging could only be performed ex vivo, on excised lungs; however, the findings still provide a clear demonstration of the effect of antiviral therapy (Figure 10). A

GFP-encoding SARS coronavirus has also been constructed, but luciferase-encoding coronaviruses have not been described [33, 78]. Of interest, BLI can also be used to study the bacterial pneumonia that often accompanies viral infection of the respiratory tract. By inserting a *lux* operon into the genome of *Streptococcus pneumoniae*, researchers were able to image pulmonary bacterial replication and demonstrate that pneumonia was more severe in mice that had undergone preliminary influenza virus infection than in control animals [79].

In addition to using BLI to visualize pathogen replication, it can also be used to study host responses to infection, by creating reporter mice, in which a luciferase gene is inserted into the animal's genome under the control of a promoter of interest [80]. For example, mice in which luciferase expression is driven by the IFN- β promoter have been used to characterize type I IFN responses to wild-type and recombinant influenza A viruses, (Figure 11) [22, 81]. Thus, BLI makes it possible to perform a variety of studies that could serve as proofs of concept for further investigation in large animals and in humans.

CONCLUSION

Molecular imaging has the potential to complement traditional radiographic methods, by characterizing pathophysiologic processes that underly pulmonary structural changes and impaired respiratory function during the course of illness. SPECT, PET, MRI, and BLI offer molecular imaging techniques that could potentiate the discovery of new biomarkers for predicting disease progression and supporting the development of novel therapies targeting viral replication or damaging host responses. Although new diseases, such as novel H1N1 influenza and SARS, will inevitably continue to emerge, molecular imaging can help to reduce their impact on public health by elucidating their pathogenetic mechanisms.

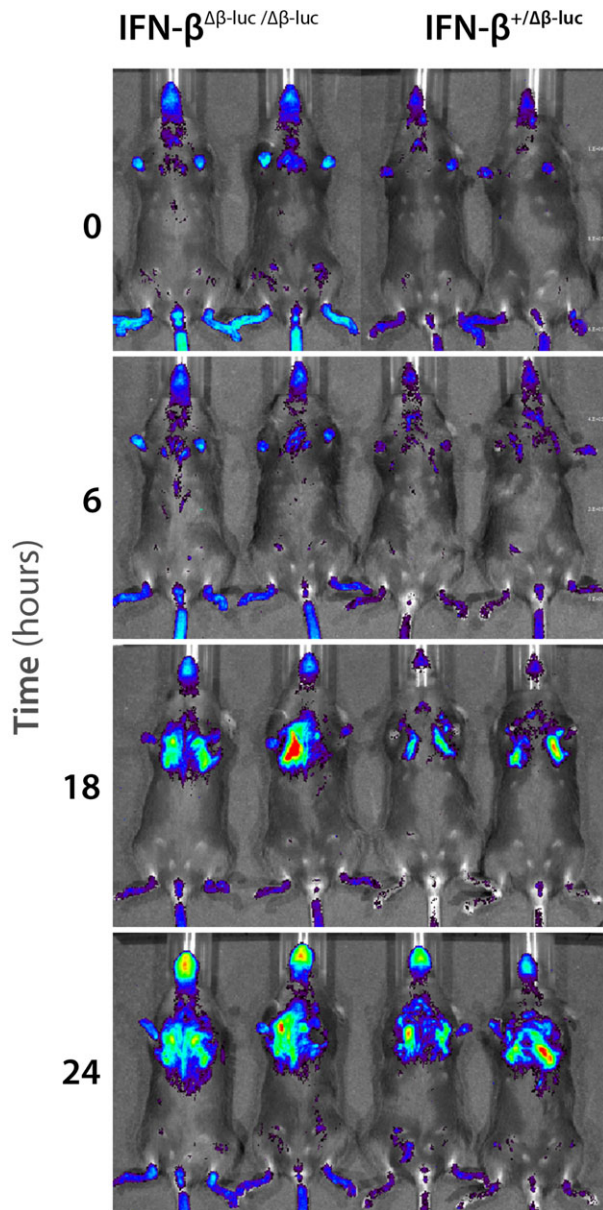


Figure 11. Response of "reporter mice" homozygous (left) or heterozygous (right) for firefly luciferase under the control of an IFN- β promoter to infection with an NS1-deficient influenza A virus. Red indicates the highest and blue the lowest level of photon flux. (From [81], with permission.)

Acknowledgments

We thank Adolfo Garcia-Sastre, King Li, and Jim Musser, for useful discussions, and Giacomo Bellani, Bernd Ebner, and Narinder Paul, for providing images.

References

1. Antonio GE, Ooi CG, Wong KT, et al. Radiographic-clinical correlation in severe acute respiratory syndrome: study of 1373 patients in Hong Kong. *Radiology* **2005**; 237:1081–90.

2. Paul NS, Chung T, Konen E, et al. Prognostic significance of the radiographic pattern of disease in patients with severe acute respiratory syndrome. *AJR Am J Roentgenol* **2004**; 182:493–8.
3. Qureshi NR, Hien TT, Farrar J, Gleeson FV. The radiologic manifestations of H5N1 avian influenza. *J Thorac Imaging* **2006**; 21:259–64.
4. Aviram G, Bar-Shai A, Sosna J, et al. H1N1 influenza: initial chest radiographic findings in helping predict patient outcome. *Radiology* **2010**; 255:252–9.

5. Semionov A, Tremblay C, Samson L, Chandonnet M, Chalaoui J, Chartrand-Lefebvre C. Pandemic influenza A (H1N1) 2009: chest radiographic findings from 147 proven cases in the Montreal area. *Can Assoc Radiol J* **2010**; 61:233–40.
6. Medicine ABoN. What is molecular imaging. <http://www.abnm.org/index.cfm?PageID=5054&RPID=5038>. Accessed 28 February 2011.
7. Mankoff DA. A definition of molecular imaging. *J Nucl Med* **2007**; 48:18N–21N.
8. Thakur M, Lentle BC. Report of a summit on molecular imaging. *Radiology* **2005**; 236:753–5.
9. Mollura DJ, Morens DM, Taubenberger JK, Bray M. The role of radiology in influenza: novel H1N1 and lessons learned from the 1918 pandemic. *J Am Coll Radiol* **2010**; 79:690–7.
10. Kim EA, Lee KS, Primack SL, et al. Viral pneumonias in adults: radiologic and pathologic findings. *Radiographics* **2002**; 22:Spec No:S137–49.
11. Fujita J, Bandoh S, Yamaguchi M, Higa F, Tateyama M. Chest CT findings of influenza virus-associated pneumonia in 12 adult patients. *Influenza Other Respi Viruses* **2007**; 1:183–7.
12. Gill JR, Sheng ZM, Ely SF, et al. Pulmonary pathologic findings of fatal 2009 pandemic influenza A/H1N1 viral infections. *Arch Path Lab Med* **2009**; 134:235–43.
13. Perez-Padilla R, de la Rosa-Zamboni D, Ponce de Leon S, et al. Pneumonia and respiratory failure from swine-origin influenza A (H1N1) in Mexico. *N Engl J Med* **2009**; 361:680–9.
14. Mollura DJ, Asnis D, Conetta R, et al. Imaging findings in a fatal case of pandemic swine-origin influenza A (H1N1). *Am J Radiol* **2009**; 193:1500–3.
15. Morens DM, Taubenberger JK, Fauci AS. Predominant role of bacterial pneumonia as a cause of death in pandemic influenza: implications for pandemic influenza preparedness. *J Infect Dis* **2008**; 198:962–70.
16. Paul NS, Roberts H, Butany J, et al. Radiologic pattern of disease in patients with severe acute respiratory syndrome: the Toronto experience. *Radiographics* **2004**; 24:553–63.
17. Ketai L, Paul NS, Wong KT. Radiology of severe acute respiratory syndrome (SARS): the emerging pathologic-radiologic correlates of an emerging disease. *J Thorac Imaging* **2006**; 21:276–83.
18. Lawler JV, Endy TP, Hensley LE, et al. *Cynomolgus macaque as an animal model for severe acute respiratory syndrome. PLoS Med* **2006**; 3:e149.
19. de Jong MD, Simmons CP, Thanh TT, et al. Fatal outcome of human influenza A (H5N1) is associated with high viral load and hypercytokinemia. *Nat Med* **2006**; 12:1203–7.

20. Palestro CJ, Love C, Miller TT. Diagnostic imaging tests and microbial infections. *Cell Microbiol* **2007**; 9:2323–33.
21. Blankenberg FG. Imaging the molecular signatures of apoptosis and injury with radiolabeled annexin V. *Proc Am Thorac Soc* **2009**; 6:469–76.
22. Kochs G, Martinez-Sobrido L, Lienenklaus S, Weiss S, Garcia-Sastre A, Staeheli P. Strong interferon-inducing capacity of a highly virulent variant of influenza A virus strain PR8 with deletions in the NS1 gene. *J Gen Virol* **2009**; 90:2990–4.
23. Oyen WJ, Claessens RA, van der Meer JW, Rubin RH, Strauss HW, Corstens FH. Indium-111-labeled human nonspecific immunoglobulin G: a new radiopharmaceutical for imaging infectious and inflammatory foci. *Clin Infect Dis* **1992**; 14:1110–8.
24. Love C, Tomas MB, Tronco GG, Palestro CJ. FDG PET of infection and inflammation. *Radiographics* **2005**; 25:1357–68.
25. Beduneau A, Ma Z, Grotepas CB, et al. Facilitated monocyte-macrophage uptake and tissue distribution of superparamagnetic iron-oxide nanoparticles. *LoS One* **2009**; 4:e4343.
26. Bulte JW, Kraitchman DL. Iron oxide MR contrast agents for molecular and cellular imaging. *NMR Biomed* **2004**; 17:484–99.
27. Rossin R, Muro S, Welch MJ, Muzykantov VR, Schuster DP. In vivo imaging of ⁶⁴Cu-labeled polymer nanoparticles targeted to the lung endothelium. *J Nucl Med* **2008**; 49:103–11.
28. Malviya G, Conti F, Chianelli M, Scopinaro F, Dierckx RA, Signore A. Molecular imaging of rheumatoid arthritis by radiolabelled monoclonal antibodies: new imaging strategies to guide molecular therapies. *Eur J Nucl Med Mol Imaging* **2010**; 37:386–98.
29. Reynolds PR, Larkman DJ, Haskard DO, et al. Detection of vascular expression of E-selectin in vivo with MR imaging. *Radiology* **2006**; 241:469–76.
30. Davis SL, Be NA, Lamichhane G, et al. Bacterial thymidine kinase as a non-invasive imaging reporter for Mycobacterium tuberculosis in live animals. *PLoS One* **2009**; 4:e6297.
31. Manicassamy B, Manicassamy S, Belichavillanueva A, Pisanelli G, Pulendran B, Garcia-Sastre A. Analysis of in vivo dynamics of influenza virus infection in mice using a GFP reporter virus. *Proc Natl Acad Sci U S A* **2010**; 107:11531–6.
32. Kittel C, Sereinig S, Ferko B, et al. Rescue of influenza virus expressing GFP from the NS1 reading frame. *Virology* **2004**; 324:67–73.
33. de Haan CA, Haijema BJ, Boss D, Heuts FW, Rottier PJ. Coronaviruses as vectors: stability of foreign gene expression. *J Virol* **2005**; 79:12742–51.
34. Beigel J, Bray M. Current and future antiviral therapy of severe seasonal and avian influenza. *Antiviral Res* **2008**; 78: 91–102.
35. Bosch BJ, Martina BE, Van Der Zee R, et al. Severe acute respiratory syndrome coronavirus (SARS-CoV) infection inhibition using spike protein heptad repeat-derived peptides. *Proc Natl Acad Sci U S A* **2004**; 101:8455–60.
36. Golda A, Pyrc K. Recent antiviral strategies against human coronavirus-related respiratory illnesses. *Curr Opin Pulm Med* **2008**; 14:248–53.
37. Yeung KS, Meanwell NA. Recent developments in the virology and antiviral research of severe acute respiratory syndrome coronavirus. *Infect Disord Drug Targets* **2007**; 7:29–41.
38. Chen DL, Bedient TJ, Kozlowski J, et al. [¹⁸F]fluorodeoxyglucose positron emission tomography for lung antiinflammatory response evaluation. *Am J Respir Crit Care Med* **2009**; 180:533–9.
39. Chen DL, Rosenbluth DB, Mintun MA, Schuster DP. FDG-PET imaging of pulmonary inflammation in healthy volunteers after airway instillation of endotoxin. *J Appl Physiol* **2006**; 100:1602–9.
40. Chen DL, Schuster DP. Positron emission tomography with [¹⁸F]fluorodeoxyglucose to evaluate neutrophil kinetics during acute lung injury. *Am J Physiol Lung Cell Mol Physiol* **2004**; 286:L834–40.
41. Abraham E. Neutrophils and acute lung injury. *Crit Care Med* **2003**; 31:S195–9.
42. Taubenberger JK, Morens DM. The pathology of influenza virus infections. *Annu Rev Pathol* **2008**; 3:499–522.
43. Tumpey TM, Garcia-Sastre A, Taubenberger JK, et al. Pathogenicity of influenza viruses with genes from the 1918 pandemic virus: functional roles of alveolar macrophages and neutrophils in limiting virus replication and mortality in mice. *J Virol* **2005**; 79:14933–4.
44. Chu YK, Ali GD, Jia F, et al. The SARS-CoV ferret model in an infection-challenge study. *Virology* **2008**; 374:151–63.
45. Perrone LA, Plowden JK, Garcia-Sastre A, Katz JM, Tumpey TM. H5N1 and 1918 pandemic influenza virus infection results in early and excessive infiltration of macrophages and neutrophils in the lungs of mice. *PLoS Pathol* **2008**; 4:e1000115.
46. Memoli MJ, Tumpey TM, Jagger BW, et al. An early 'classical' swine H1N1 influenza virus shows similar pathogenicity to the 1918 pandemic virus in ferrets and mice. *Virology* **2009**; 393:338–45.
47. Kash JC. Applications of high-throughput genomics to antiviral research: evasion of antiviral responses and activation of inflammation during fulminant RNA virus infection. *Antiviral Res* **2009**; 83:10–20.
48. Zheng BJ, Chan KW, Lin YP, et al. Delayed antiviral plus immunomodulator treatment still reduces mortality in mice infected by high inoculum of influenza A/H5N1 virus. *Proc Natl Acad Sci U S A* **2008**; 105:8091–6.
49. Simmons C, Farrar J. Insights into inflammation and influenza. *N Engl J Med* **2008**; 359:1621–3.
50. Fedson DS. Confronting the next influenza pandemic with anti-inflammatory and immunomodulatory agents: why they are needed and how they might work. *Influenza Other Respi Viruses* **2009**; 3:129–42.
51. Salomon R, Hoffmann E, Webster RG. Inhibition of the cytokine response does not protect against lethal H5N1 influenza infection. *Proc Natl Acad Sci U S A* **2007**; 104:12479–81.
52. Bellani G, Guerra L, Pesenti A, Messa C. Imaging of lung inflammation during severe influenza A: H1N1. *Intensive Care Med* **2010**; 36:717–8.
53. Bellani G, Messa C, Guerra L, et al. Lungs of patients with acute respiratory distress syndrome show diffuse inflammation in normally aerated regions: a [¹⁸F]-fluoro-2-deoxy-D-glucose PET/CT study. *Crit Care Med* **2009**; 37:2216–22.
54. Rini JN, Palestro CJ. Imaging of infection and inflammation with ¹⁸F-FDG-labeled leukocytes. *Q J Nucl Med Mol Imaging* **2006**; 50:143–6.
55. Locke LW, Chordia MD, Zhang Y, et al. A novel neutrophil-specific PET imaging agent: cFLFLFK-PEG-⁶⁴Cu. *J Nucl Med* **2009**; 50:790–7.
56. Gambhir SS, Herschman HR, Cherry SR, et al. Imaging transgene expression with radionuclide imaging technologies. *Neoplasia* **2000**; 2:118–38.
57. Brader P, Kelly K, Gang S, et al. Imaging of lymph node micrometastases using an oncolytic herpes virus and [¹⁸F]FEAU PET. *PLoS One* **2009**; 4:e4789.
58. Price RW, Saito Y, Fox JJ. Prospects for the use of radiolabeled antiviral drugs in the diagnosis of herpes simplex encephalitis. *Biochem Pharmacol* **1983**; 32:2455–61.
59. Buursma AR, de Vries EF, Garssen J, et al. [¹⁸F]FHPG positron emission tomography for detection of herpes simplex virus (HSV) in experimental HSV encephalitis. *J Virol* **2005**; 79:7721–7.
60. Bergstrom M, Cass LM, Valind S, et al. Deposition and disposition of [¹¹C]zanamivir following administration as an intranasal spray. Evaluation with positron emission tomography. *Clin Pharmacokinet* **1999**; 36(Suppl. 1):33–9.
61. Hatori A, Arai T, Yanamoto K, et al. Biodistribution and metabolism of the anti-influenza drug [¹¹C]oseltamivir and its active metabolite [¹¹C]Ro 64-0802 in mice. *Nucl Med Biol* **2009**; 36:47–55.
62. Walker RC, Jones-Jackson LB, Martin W, Habibian MR, Delbeke D. New imaging tools for the diagnosis of infection. *Future Microbiol* **2007**; 2:527–54.

63. Garbow JR, Wang M, Wang Y, Lubet RA, You M. Quantitative monitoring of adenocarcinoma development in rodents by magnetic resonance imaging. *Clin Cancer Res* **2008**; 14:1363–7.
64. Garbow JR, Zhang Z, You M. Detection of primary lung tumors in rodents by magnetic resonance imaging. *Cancer Res* **2004**; 64:2740–2.
65. Beckmann N, Karmounty Quintana H, Ble FX, et al. Magnetic resonance imaging (MRI) of the lung as a tool for the non-invasive evaluation of drugs in rat models of airways diseases. *ALTEX* **2006**; 23:420–8.
66. Eibel R, Herzog P, Dietrich O, et al. Pulmonary abnormalities in immunocompromised patients: comparative detection with parallel acquisition MR imaging and thin-section helical CT. *Radiology* **2006**; 241:880–91.
67. Ebner B, Behm P, Jacoby C, et al. Early assessment of pulmonary inflammation by 19F MRI in vivo. *Circ Cardiovasc Imaging* **2010**; 3:202–10.
68. Marzola P, Lanzoni A, Nicolato E, et al. (1)H MRI of pneumococcal pneumonia in a murine model. *J Magn Reson Imaging* **2005**; 22:170–4.
69. Tournebise R, Doan BT, Dillies MA, Maurin S, Beloeil JC, Sansonetti PJ. Magnetic resonance imaging of *Klebsiella pneumoniae*-induced pneumonia in mice. *Cell Microbiol* **2006**; 8:33–43.
70. Olsson LE, Smailagic A, Onnervik PO, Hockings PD. (1)H and hyperpolarized (3)He MR imaging of mouse with LPS-induced inflammation. *J Magn Reson Imaging* **2009**; 29:977–81.
71. Dou H, Destache CJ, Morehead JR, et al. Development of a macrophage-based nanoparticle platform for antiretroviral drug delivery. *Blood* **2006**; 108:2827–35.
72. Dou H, Morehead J, Destache CJ, et al. Laboratory investigations for the morphologic, pharmacokinetic, and anti-retroviral properties of indinavir nanoparticles in human monocyte-derived macrophages. *Virology* **2007**; 358:148–58.
73. Himmelreich U, Dresselaers T. Cell labeling and tracking for experimental models using magnetic resonance imaging. *Methods* **2009**; 48:112–24.
74. Hutchens M, Luker GD. Applications of bioluminescence imaging to the study of infectious diseases. *Cell Microbiol* **2007**; 9:2315–22.
75. Luker KE, Hutchens M, Schultz T, Pekosz A, Luker GD. Bioluminescence imaging of vaccinia virus: effects of interferon on viral replication and spread. *Virology* **2005**; 341:284–300.
76. Luker KE, Luker GD. Applications of bioluminescence imaging to antiviral research and therapy: multiple luciferase enzymes and quantitation. *Antiviral Res* **2008**; 78:179–87.
77. Zaitseva M, Kapnick SM, Scott J, et al. Application of bioluminescence imaging to the prediction of lethality in vaccinia virus-infected mice. *J Virol* **2009**; 83:10437–7.
78. Sims AC, Burkett SE, Yount B, Pickles RJ. SARS-CoV replication and pathogenesis in an in vitro model of the human conducting airway epithelium. *Virus Res* **2008**; 133:33–44.
79. Smith MW, Schmidt JE, Rehg JE, Orihuela CJ, McCullers JA. Induction of pro- and anti-inflammatory molecules in a mouse model of pneumococcal pneumonia after influenza. *Comp Med* **2007**; 57:82–9.
80. Luker KE, Luker GD. Bioluminescence imaging of reporter mice for studies of infection and inflammation. *Antiviral Res* **2010**; 86:93–100.
81. Lienenklaus S, Cornitescu M, Zietara N, et al. Novel reporter mouse reveals constitutive and inflammatory expression of IFN-beta in vivo. *J Immunol* **2009**; 183:3229–36.